

Equilibrium Water Partial Pressures and Salt Solubilities in Aqueous NH_4HSO_4 to Low Temperatures

Yan Yao,^{†,‡} Mario Massucci,[§] Simon L. Clegg,^{*,§} and Peter Brimblecombe[§]

School of Environmental Sciences, University of East Anglia, Norwich NR4 7TJ, U.K., and
Institute of Salt Lakes, Chinese Academy of Sciences, Xi'an 710043, China

Received: November 6, 1998

Equilibrium water partial pressures ($p_{\text{H}_2\text{O}}$) above 3.69₅, 5.67₂, and 8.65₁ mol kg⁻¹ $\text{NH}_4\text{HSO}_{4(\text{aq})}$, and 10.19 mol kg⁻¹ $\text{H}_2\text{SO}_{4(\text{aq})}$, have been determined using a capacitance manometer over the temperature ranges 288.1₁–239.5₆ K and 298.1₂–238.5₂ K, respectively. Measured $p_{\text{H}_2\text{O}}$ above the aqueous H_2SO_4 solution agree with values calculated using the model of Clegg et al. (*J. Phys. Chem. A* 1998, 102, 2137–2154) to within +5.3% to -2.8% at all temperatures. Results for the $\text{NH}_4\text{HSO}_{4(\text{aq})}$ solutions are also consistent with calculated $p_{\text{H}_2\text{O}}$, with deviations of +0.45% to +6.27% (measured - calculated) for all data. The formation of solids was observed in the $\text{NH}_4\text{HSO}_{4(\text{aq})}$ solutions at the following temperatures: 258.0₆ ± 0.1 K [3.69₅ mol kg⁻¹], 246.4₇ ± 0.1 K [5.67₂ mol kg⁻¹], and 261.0₁ ± 0.1 K [8.65₁ mol kg⁻¹]. The data are consistent with predictions of ice precipitation in the 3.69₅ mol kg⁻¹ test solution, letovicite ($(\text{NH}_4)_3\text{H}(\text{SO}_4)_2(\text{cr})$) in the 8.65₁ mol kg⁻¹ solution, and both ice and letovicite in the 5.67₂ mol kg⁻¹ solution. The liquid-phase compositions of the solutions containing precipitates are calculated for different temperatures. The results of the experiments are compared with solubility data from other studies and with model predictions of solid/liquid equilibrium for NH_4HSO_4 – H_2SO_4 – H_2O mixtures to low temperature over a wide range of composition.

1. Introduction

Acidic ammonium sulfate aerosols in the troposphere form cloud condensation nuclei, affect visibility, and are also an important component of urban aerosols.¹ To predict their properties, we have recently developed a multicomponent mole-fraction-based thermodynamic model of the H^+ – NH_4^+ – SO_4^{2-} – NO_3^- – H_2O system to low temperatures.² This is based on aqueous activity and solubility measurements, including data for supersaturated solutions from single-particle experiments (e.g., see Tang and Munkelwitz³). However, for H^+ – NH_4^+ – SO_4^{2-} – H_2O mixtures the model is largely dependent on data for temperatures of ≥ 273.15 K.

Recently, Imre et al.⁴ have investigated the low temperature solid/liquid phase equilibrium of aqueous NH_4HSO_4 using levitated single particles. At relatively low molalities (<5.79 mol kg⁻¹, or 40 mass %) the phase diagram determined by Imre et al.⁴ (see their Figure 4) differs significantly from that predicted by the model of Clegg et al.² In particular, there is a large disagreement in the freezing points with respect to ice, which implies differences in the variation of water activity of the solutions with temperature. At higher molalities Imre et al.⁴ obtain $\text{NH}_4\text{HSO}_{4(\text{cr})}$ as the precipitating solid phase, whereas data from bulk experiments⁵ yield $(\text{NH}_4)_3\text{H}(\text{SO}_4)_2(\text{cr})$ (letovicite) for temperatures below about 303 K. We have therefore measured equilibrium water partial pressures above 3.69₅–8.65₁ mol kg⁻¹ $\text{NH}_4\text{HSO}_{4(\text{aq})}$ (or 29.8–49.89 mass %), and determined the temperatures at which solid phases precipitate in the solutions, to resolve these discrepancies and to define better the thermodynamic properties of $\text{NH}_4\text{HSO}_{4(\text{aq})}$ solutions at low temperature. The experiments are described below and the

results compared with those of Imre et al.⁴ and with predictions of the model of Clegg et al.² They are also discussed in the broader context of solid/liquid equilibrium in acid ammonium sulfate systems.

2. Experiments

Equilibrium pressures of water were measured using the method described by Massucci et al.⁶ in which the pressure over an aqueous test solution, which has been previously degassed to remove dissolved air, is determined directly at a known temperature using a capacitance manometer.

The molalities of the test $\text{NH}_4\text{HSO}_{4(\text{aq})}$ solutions were chosen in order to investigate the composition region likely to remain liquid to the lowest temperatures. The molalities were also selected such that saturation with respect to both ice and/or one of the acid ammonium salts would be attained as temperature was decreased. This is illustrated in Figure 1, which shows the temperature and composition ranges of the measurements, together with the saturation curves for ice and letovicite predicted by the model of Clegg et al.²

Equilibrium water partial pressures above a 10.19 mol kg⁻¹ $\text{H}_2\text{SO}_{4(\text{aq})}$ solution were also measured, over a 2 order of magnitude range of partial pressure, as a test of the experimental technique.

(a) Apparatus. The experimental setup is shown in Figure 2 and consists of a twin-walled glass cell connected to a vacuum line, thermostatic bath, and manometer. Vapor pressures were measured using a capacitance gauge (Edwards Barocell model 655, 0–10 Torr range), which was maintained at a constant 45 °C operating temperature. Its 0–10 V output was checked against a direct-current millivolt source of $\pm 0.05\%$ accuracy. The cell was evacuated using a series combination of rotary and diffusion pumps capable of maintaining pressures down to 10^{-6} Torr (133.3×10^{-6} Pa).

[†] Chinese Academy of Sciences.

[‡] Visiting Scholar at the School of Environmental Sciences.

[§] University of East Anglia.

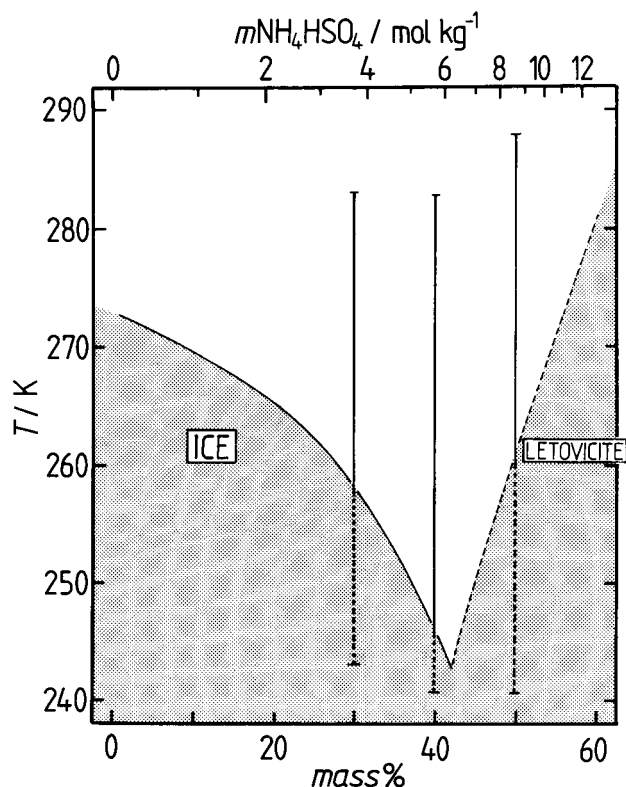


Figure 1. Range of temperatures (T) over which partial pressures were measured for each of the aqueous NH_4HSO_4 test solutions. Saturation with respect to ice and letovicite, calculated using the model of Clegg et al.,² is also shown. Note that, for temperatures below the saturation curves, the compositions of the test solutions are altered by the precipitation of solids. The dashed elements of the lines for the three test solutions therefore do not represent the aqueous-phase compositions for those temperatures (see section 3.c).

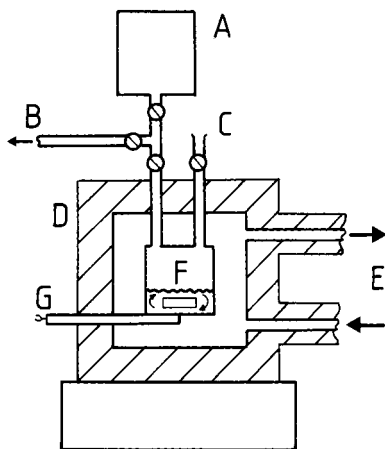


Figure 2. Schematic diagram of the apparatus: A, pressure gauge; B, connection to vacuum line; C, inlet for weighed solution samples; D, test cell with thermal insulation; E, connections to refrigerating bath/circulator; F, test solution with magnetic stirring bar; G, platinum resistance thermometer.

The temperature of the solution in the cell was maintained by a Julabo FP 30 bath/recirculator, which passed ethanol coolant between the cell walls and controlled the temperature to a precision of about ± 0.02 K. The temperature of the cell during experimental runs was monitored by a separate platinum resistance probe located between the cell walls near the solution. The bath temperature was similarly monitored. The probes were previously calibrated against both the internal temperature sensor

TABLE 1: Measured Equilibrium Partial Pressures of Water ($p_{\text{H}_2\text{O}}$) above 10.19 mol kg^{-1} Aqueous H_2SO_4

T (K)	$p_{\text{H}_2\text{O}}$ (Pa)	n^a	T (K)	$p_{\text{H}_2\text{O}}$ (Pa)	n^a
241.0(8)	11.20	4	268.3(8)	140.0	6
244.0(5)	15.55	4	240.9(5)	11.09	7
253.8(0)	39.52	4	298.0(0)	1126	7
263.5(3)	92.77	4	240.9(6)	11.04	7
273.2(7)	202.9	4	253.5(9)	37.90	7
241.1(3)	11.21	5	273.1(2)	198.5	7
248.8(8)	24.77	5	244.0(6)	14.88	7
258.6(4)	60.34	5	293.1(5)	817.6	7
273.3(2)	207.0	5	263.5(5)	90.56	7
283.2(0)	424.3	5	253.5(9)	39.42	5
298.0(6)	1141	5	238.5(2)	9.19	5
241.1(2)	11.13	6	243.7(2)	15.23	5
298.1(2)	1132	6	253.5(3)	38.55	5
288.1(8)	592.0	6	273.3(7)	200.2	5

^a Number of degassing cycles before pressure measurement.

in the bath and standard thermometers and had an accuracy of about ± 0.1 K. The capacitance manometer and thermometers monitoring the thermostatic bath and the cell were connected to a personal computer via a 16 bit A/D converter (Pico Technology Pico ADC-16), with measurements taken at 1 min intervals. The A/D converter was set to 14 bits when recording temperatures, which resulted in an indicated resolution of 0.015 K. A higher resolution (16 bits) was used for recording the output from the manometer so that pressure measurements could be resolved to 0.015% of the full scale reading, equivalent to 0.2 Pa.

(b) Materials. A stock solution of H_2SO_4 was prepared by diluting 98% commercial acid (BDH, Aristar grade) using laboratory-distilled water. The molality of the aqueous H_2SO_4 was determined by acidimetric titration against aqueous sodium hydroxide (Aldrich Volumetric Standard), which was confirmed by gravimetric titration against $\text{KHC}_6\text{H}_4(\text{COO})_2$ (A.C.S. Acidimetric Standard). Three samples of each solution were titrated, with a reproducibility of $\pm 0.05\%$.

BDH Analar grade $(\text{NH}_4)_2\text{SO}_4$ (>99.5%) was dried to constant weight and used without further treatment.

The $8.651 \text{ mol kg}^{-1}$ NH_4HSO_4 test solution was prepared by weighing diluted H_2SO_4 stock solution and $(\text{NH}_4)_2\text{SO}_4$ solid to a molality ratio of 1:1 (± 0.005), using a balance with an accuracy of $\pm 1 \times 10^{-4}$ g. The lower molality solutions (5.672 and $3.695 \text{ mol kg}^{-1}$) were prepared by dilution (see below).

(c) Procedure. About 40 cm^3 of test solution was added to the cell at room temperature and then cooled to 240 K (close to the lower limit of the bath/recirculator). At this temperature the cell was evacuated slowly to prevent explosive decompression of the dissolved air and then warmed to room temperature to release further dissolved gas. The degassing process was repeated about four times until the pressure in the vacuum line was maintained at about 5×10^{-4} Pa, and there was no change in the observed vapor pressure above the solution at low temperature when the cell was isolated. The cell was then allowed to stabilize for at least 2 h and the vapor pressure measured when equilibrium with respect to temperature and pressure was achieved. After each measurement the temperature was reset. To observe accurately the onset of precipitation and to measure the vapor pressure over the saturated or near-saturated solutions, temperature intervals of 0.2 K or less were used.

The two lower molality NH_4HSO_4 test solutions were produced in the cell by the addition of known masses of water to the solution already present. The degassing procedure was repeated after each of the additions. Calculations suggest that

TABLE 2: Measured Equilibrium Partial Pressures of Water ($p_{\text{H}_2\text{O}}$) above Aqueous NH_4HSO_4 Solutions

$m\text{NH}_4\text{HSO}_4^a$ (mol kg ⁻¹)	T (K)	$p_{\text{H}_2\text{O}}$ (Pa)	prec ^b	a_w^c	$m\text{NH}_4^{+d}$ (mol kg ⁻¹)	$m\text{H}^{+d}$ (mol kg ⁻¹)	$\text{H}_2\text{O}_{(\text{cr})}^e$ (mol)	$(\text{NH}_4)_3\text{H}(\text{SO}_4)_2(\text{cr})^e$ (mol)
3.69(5)	283.1(5)	1096		0.8929				
3.69(5)	278.1(2)	780.3		0.8967				
3.69(5)	275.1(9)	631.1		0.8920				
3.69(5)	273.2(2)	547.2		0.8915				
3.69(5)	271.1(7)	472.2		0.8939				
3.69(5)	268.2(4)	377.7		0.8902				
3.69(5)	265.2(0)	301.1		0.8959				
3.69(5)	263.3(0)	257.9		0.8905				
3.69(5)	261.3(2)	219.4		0.8869				
3.69(5)	258.4(3)	171.9		0.8789				
3.69(5)	258.1(3)	168.7		0.8842				
3.69(5)	258.0(6)	166.6	*f	0.8782	3.750	3.750	0.807	0.0
3.69(5)	257.3(1)	156.7	*	0.8790	3.889	3.889	2.771	0.0
3.69(5)	256.3(2)	142.7	*	0.8694	4.070	4.070	5.109	0.0
3.69(5)	243.5(7)	39.82	*	0.7528	6.183	6.183	22.34	0.0
5.67(2)	283.0(6)	1000		0.8196				
5.67(2)	280.1(7)	816.2		0.8139				
5.67(2)	278.1(0)	710.0		0.8170				
5.67(2)	275.2(5)	574.5		0.8085				
5.67(2)	273.2(6)	498.0		0.8090				
5.67(2)	273.2(4)	497.0		0.8085				
5.67(2)	268.2(3)	342.1		0.8069				
5.67(2)	263.3(4)	232.4		0.7999				
5.67(2)	263.3(1)	232.3		0.8015				
5.67(2)	258.3(2)	155.1		0.8002				
5.67(2)	255.3(4)	120.7		0.7987				
5.67(2)	253.3(7)	102.3		0.8008				
5.67(2)	247.9(5)	62.89		0.7940				
5.67(2)	246.9(5)	57.50		0.7949				
5.67(2)	246.6(7)	55.68		0.7897				
5.67(2)	246.4(7)	54.01	*f	0.7801	5.718	5.718	0.4443	0.0
5.67(2)	245.4(8)	48.83	*	0.7726	5.877	5.877	1.932	0.0
5.67(2)	243.5(0)	40.34	*	0.7677	6.194	6.194	4.678	0.0
5.67(2)	240.5(9)	30.81 ^s	*	0.7739	5.652	6.978	14.30	0.4921
5.67(2)	240.5(5)	30.60 ^s	*	0.7716	5.642	6.989	14.42	0.4985
5.67(2)	240.5(3)	29.70 ^s	*	0.7503	5.637	6.995	14.48	0.5018
8.65(1)	288.1(1)	1231		0.7240				
8.65(1)	283.1(4)	885.1		0.7216				
8.65(1)	283.1(3)	885.1		0.7220				
8.65(1)	280.1(4)	721.5		0.7209				
8.65(1)	278.2(8)	627.8		0.7134				
8.65(1)	273.1(9)	438.7		0.7163				
8.65(1)	273.1(9)	438.3		0.7156				
8.65(1)	270.2(9)	351.1		0.7095				
8.65(1)	268.2(2)	302.0		0.7128				
8.65(1)	267.2(7)	280.0		0.7104				
8.65(1)	265.3(2)	239.5		0.7060				
8.65(1)	265.2(8)	239.4		0.7079				
8.65(1)	264.2(4)	221.8		0.7113				
8.65(1)	263.3(5)	205.3		0.7061				
8.65(1)	263.2(9)	204.7		0.7074				
8.65(1)	262.4(0)	189.3		0.7019				
8.65(1)	262.3(7)	189.5		0.7044				
8.65(1)	261.3(0)	174.3		0.7057				
8.65(1)	261.0(1)	171.0	*h	0.7087	8.637	8.646	0.0	0.0046
8.65(1)	260.3(2)	161.6	*	0.7081	8.517	8.606	0.0	0.0447
8.65(1)	259.3(1)	149.4	*	0.7107	8.342	8.548	0.0	0.1031
8.65(1)	258.3(5)	138.0	*	0.7103	8.177	8.493	0.0	0.1581
8.65(1)	240.4(6)	28.92	*	0.7356	5.409	7.570	0.0	1.081
8.65(1)	240.6(0)	29.75	*	0.7465	5.428	7.577	0.0	1.074
8.65(1)	240.4(8)	29.35	*	0.7451	5.412	7.571	0.0	1.080
8.65(1)	240.4(6)	29.50	*	0.7503	5.409	7.570	0.0	1.081
8.65(1)	240.4(0)	29.42	*	0.7527	5.401	7.568	0.0	1.083
8.65(1)	239.5(6)	25.79	*	0.7159	5.288	7.530	0.0	1.121

^a Determined by titration of solution samples withdrawn from the test cell after each series of measurements. ^b A “*” indicates those temperatures for which precipitated solids were observed in the test solutions. ^c Water activity (or equilibrium relative humidity) of the solution, equal to $p_{\text{H}_2\text{O}}/p_{\text{H}_2\text{O}}^\circ$ where $p_{\text{H}_2\text{O}}^\circ$ is the vapor pressure of pure water at the experimental temperature.⁷ ^d Calculated molalities of total aqueous H^+ and NH_4^+ present in the test solutions in which precipitates had formed. ^e Calculated moles of ice and letovicite present in the test solutions in which precipitates had formed, based upon a total water content of 1.0 kg. ^f The precipitates formed consisted of amorphous, flake-like crystals which tended to remain suspended (3.69₂ mol kg⁻¹ solution), or only settle slowly (5.67₂ mol kg⁻¹ solution) to the bottom of the cell. Crystals of a more obviously ice-like appearance were observed at temperatures about 1–3 K lower than those at which the precipitate initially formed. These observations can probably be explained in terms of the differing concentrations and temperatures at which ice formation occurs, leading to incorporation of solution elements (H_2O and ions) into what appears to be a very loose crystalline structure. The fact that the measured $p_{\text{H}_2\text{O}}$ values are consistent with those over ice, and that the solutions remain partially liquid on freezing, strongly suggests that no additional solid (such as a hydrate, for example) is formed. However, further experiments would be required to determine this conclusively. ^g Pressures were determined at these temperatures after the solution had been left overnight and without degassing immediately before the measurement. ^h The precipitate appeared as fine white crystals that rapidly settled to the bottom of the test cell. No ice was observed to form.

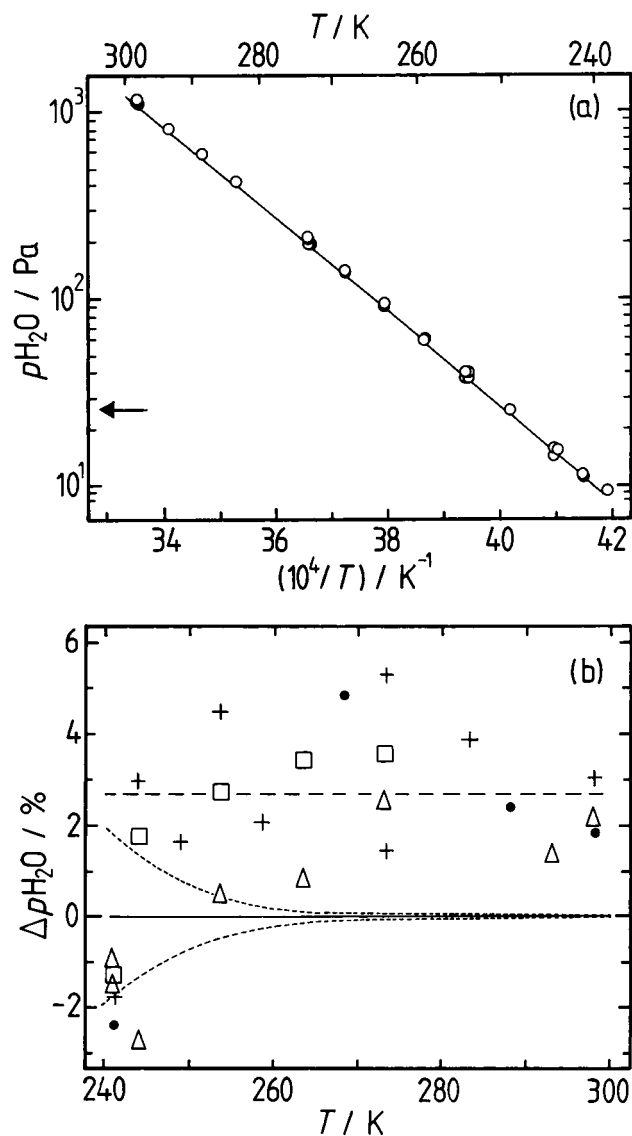


Figure 3. Equilibrium partial pressures of water ($p_{\text{H}_2\text{O}}$) above 10.19 mol kg^{-1} aqueous H_2SO_4 (49.99 mass %). (a) Symbols represent measurements in this study, and the line is calculated using the model of Clegg et al.² The horizontal arrow indicates the lower limit of $p_{\text{H}_2\text{O}}$ determined above the aqueous NH_4HSO_4 test solutions. (b) Deviation plot ($\Delta p_{\text{H}_2\text{O}} = 100[p_{\text{H}_2\text{O}}(\text{expt}) - p_{\text{H}_2\text{O}}(\text{calc})]/p_{\text{H}_2\text{O}}(\text{calc})$), also showing the number of degassing cycles carried out before each measurement: (□) four cycles; (+) five cycles; (●) six cycles; (Δ) seven cycles. The dashed line represents the mean value of $\Delta p_{\text{H}_2\text{O}}$ over the range of pressures measured above the $\text{NH}_4\text{HSO}_4(\text{aq})$ solutions. The dotted lines represent the uncertainty due to the resolution of the pressure measurements.

the loss of water from the system is small and has a negligible effect on the molality of the test solutions.

Samples of the test solutions were withdrawn from the cell after the completion of each series of measurements. These were titrated by weight with aqueous NaOH solution. The molality of the most concentrated solution (8.651 mol kg^{-1}) was confirmed to within 0.1%. Results for the other two solutions gave molalities 0.9% lower than the expected values. The most likely explanation is cumulative errors in the masses of the added water (for dilution) and, to a lesser extent, the extracted samples. The final molalities, obtained by titration of the extracted samples, are taken to be the correct ones. We note that errors of +1% in NH_4HSO_4 molality correspond to decreases in water partial pressure of only about 0.24% (5.672 mol kg^{-1} solution) and 0.15% (3.695 mol kg^{-1} solution).

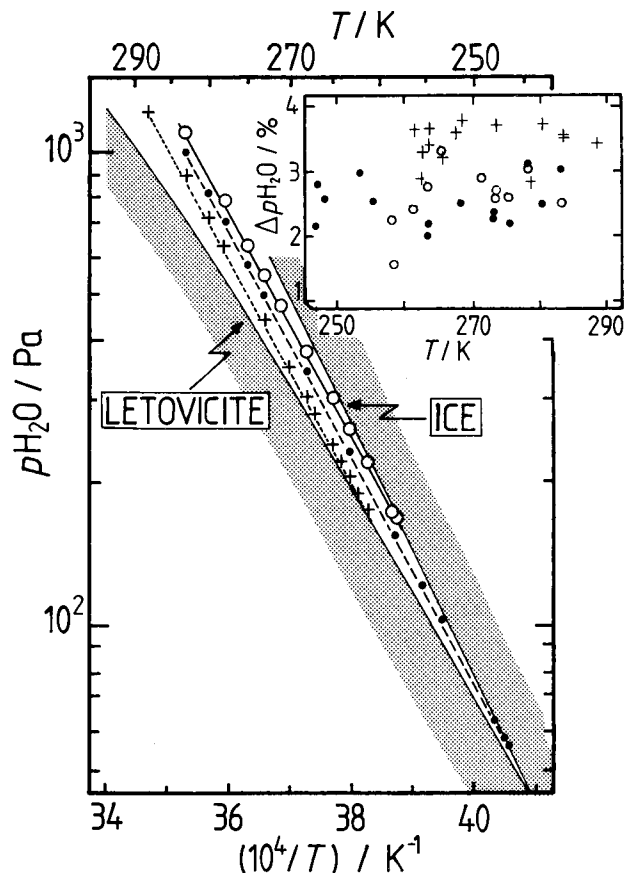


Figure 4. Equilibrium partial pressures of water ($p_{\text{H}_2\text{O}}$) above aqueous NH_4HSO_4 solutions (not containing precipitates): (○) 3.695 mol kg^{-1} ; (●) 5.672 mol kg^{-1} ; (+) 8.651 mol kg^{-1} . Lines are calculated using the model of Clegg et al.²: (solid) 3.695 mol kg^{-1} ; (dashed) 5.672 mol kg^{-1} ; (dotted) 8.651 mol kg^{-1} . Calculated values of $p_{\text{H}_2\text{O}}$ above solutions saturated with respect to ice and letovicite are indicated by the upper and lower fine solid lines. Inset: deviation plot ($\Delta p_{\text{H}_2\text{O}} = 100[p_{\text{H}_2\text{O}}(\text{expt}) - p_{\text{H}_2\text{O}}(\text{calc})]/p_{\text{H}_2\text{O}}(\text{calc})$).

3. Results

Partial pressures determined in this work are listed in Tables 1 and 2 for the aqueous H_2SO_4 and NH_4HSO_4 solutions, respectively.

(a) Aqueous H_2SO_4 . Measured and calculated equilibrium $p_{\text{H}_2\text{O}}$ over the 10.19 mol kg^{-1} solution are shown in Figure 3a. It is clear from the deviation plot (Figure 3b) that the data agree closely with partial pressures calculated theoretically.^{2,7} The mean deviation for the 25.79–1231 Pa pressure range measured over the aqueous NH_4HSO_4 solutions is $+2.72 \pm 1.4\%$, and this does not appear to vary significantly with either the number of degassing cycles or with temperature. Because the water activity of 10.19 mol kg^{-1} H_2SO_4 at 298.15 K (0.3517) is known to better than 0.5% (based on vapor pressure data)⁷ and the thermal properties of aqueous H_2SO_4 are well established,^{8,9} this deviation is attributed to a small systematic error in the measurements. A similar artifact was found in previous experiments on aqueous H_2SO_4 .⁶

(b) Aqueous NH_4HSO_4 . Measured and calculated partial pressures above the test solutions, for temperatures at which they remained fully liquid, are shown in Figure 4. The calculated values agree well with the data at each molality, with the following mean deviations: $+2.58 \pm 0.45\%$ (3.695 mol kg^{-1}), $+2.48 \pm 0.34\%$ (5.672 mol kg^{-1}), $+3.45 \pm 0.32\%$ (8.651 mol kg^{-1}). These are comparable to the deviations found for the aqueous H_2SO_4 test solution in both sign and magnitude, and

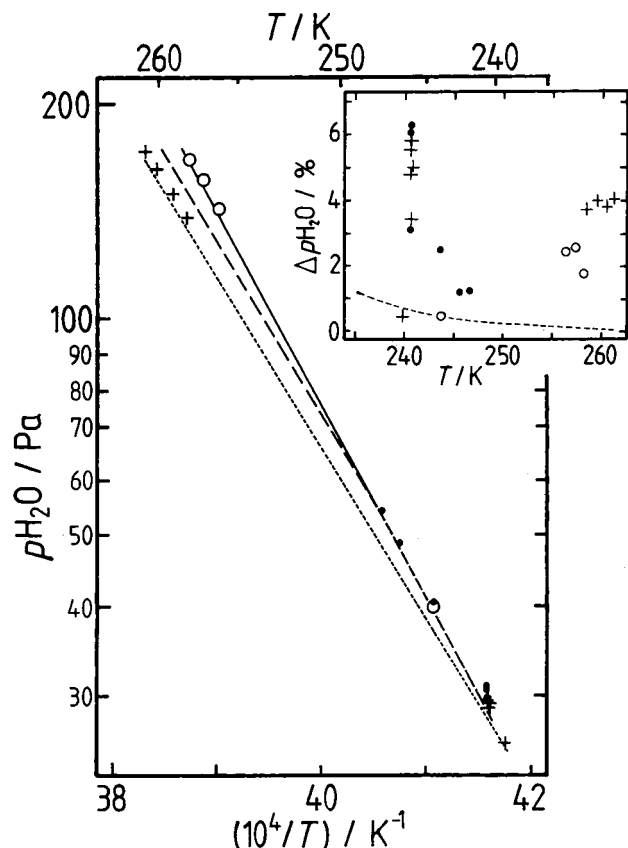


Figure 5. Equilibrium partial pressures of water ($p_{\text{H}_2\text{O}}$) above aqueous NH_4HSO_4 solutions containing precipitated solids. Initial molalities: (○) $3.69_5 \text{ mol kg}^{-1}$; (●) $5.67_2 \text{ mol kg}^{-1}$; (+) $8.65_1 \text{ mol kg}^{-1}$. Lines are calculated using the model of Clegg et al.²: (solid) $3.69_5 \text{ mol kg}^{-1}$; (dashed) $5.67_2 \text{ mol kg}^{-1}$; (dotted) $8.65_1 \text{ mol kg}^{-1}$. The calculated partial pressures take into account the changing composition of the aqueous component of the test solutions (see Table 2). Note that for $T < 246.75 \text{ K}$, the 3.69_5 and $5.67_2 \text{ mol kg}^{-1}$ test solutions are both predicted to be saturated with respect to ice; hence, the calculated $p_{\text{H}_2\text{O}}$ values are the same. Inset: deviation plot ($\Delta p_{\text{H}_2\text{O}} = 100[p_{\text{H}_2\text{O}}(\text{expt}) - p_{\text{H}_2\text{O}}(\text{calc})]/p_{\text{H}_2\text{O}}(\text{calc})$).

there is no apparent trend with temperature (see inset of Figure 4). We also note that the scatter in the available osmotic coefficient data for aqueous NH_4HSO_4 at room temperature leads to as much as a 2% uncertainty in the water activity of an $8.65_1 \text{ mol kg}^{-1}$ solution (see Figure 14 of Clegg et al.²). It is concluded that for these solution compositions and temperatures the measurements and the model of Clegg et al.² agree to within the uncertainty in the experiments.

(c) Aqueous NH_4HSO_4 (with Precipitates). Solids were first observed to form in the test solutions at the following temperatures: $258.0_6 \pm 0.1 \text{ K}$ ($3.69_5 \text{ mol kg}^{-1} \text{ NH}_4\text{HSO}_4$), $246.4_7 \pm 0.1 \text{ K}$ ($5.67_2 \text{ mol kg}^{-1} \text{ NH}_4\text{HSO}_4$), and $261.0_1 \pm 0.1 \text{ K}$ ($8.65_1 \text{ mol kg}^{-1} \text{ NH}_4\text{HSO}_4$). Neither the precipitates nor the residual aqueous solutions were analyzed. Thus, the compositions of the aqueous components of the test solutions are not known directly. They have therefore been calculated using the model of Clegg et al.² (see Table 2) together with the equilibrium $p_{\text{H}_2\text{O}}$. Measured and calculated partial pressures above the test solutions containing precipitates are plotted in Figure 5. It can be seen that the values of $\ln(p_{\text{H}_2\text{O}})$ tend to converge as temperature is decreased. This can be explained in terms of the changing composition of the aqueous phase in each of the test samples. For the 3.69_5 and $5.67_2 \text{ mol kg}^{-1}$ solutions ice is predicted to precipitate first as temperature is decreased, at 258.35 and 246.75 K , respectively. These temperatures agree

closely with the observed values, tending to confirm ice as the solid. The removal of liquid water as ice will concentrate the solutions, thus lowering the water activity and equilibrium $p_{\text{H}_2\text{O}}$. Of course, at temperatures at which both solutions contain ice (calculated as $\leq 246.75 \text{ K}$), the equilibrium $p_{\text{H}_2\text{O}}$ must necessarily be the same. The similarity of the measured partial pressures at the lowest temperatures (Figure 5) and the reduction in the water activity relative to the solutions without precipitates (Table 2) confirm this.

The appearance of the precipitates in the 3.69_5 and $5.67_2 \text{ mol kg}^{-1}$ solutions was generally similar (see notes to Table 2) and very different from that observed for the $8.65_1 \text{ mol kg}^{-1}$ solution, consistent with the analysis of the results presented here.

Letovicite is expected to be the initial solid to form in the $8.65_1 \text{ mol kg}^{-1}$ solution (e.g., see Figure 14 of Clegg et al.²), the temperature of 261.09 K predicted by the model of Clegg et al. agreeing well with the 261.3_0 – 261.0_1 K observed in the experiments. In this case, precipitation of the salt while the liquid phase remains undersaturated with respect to ice causes, first, the solution to become more dilute, thus raising its water activity and equilibrium $p_{\text{H}_2\text{O}}$. Second, the formation of letovicite, which contains a 3:1 molar ratio of NH_4^+/H^+ , causes the remaining aqueous solution to become relatively more acidic. For example, a stoichiometric composition of $(\text{NH}_4)_{0.857}\text{H}_{1.14}\text{SO}_4$ is predicted at 243 K . However, this composition change has a relatively minor influence on the partial pressure of water over the range of temperatures for which measurements were made. The overall effect is therefore to increase the partial pressure of water relative to an aqueous solution of constant ($8.65_1 \text{ mol kg}^{-1}$) molality, resulting in values similar to those for the other test solutions at the lowest temperatures measured (Figure 5).

The partial pressures of water calculated for the three solutions (with solids present) agree satisfactorily with the data, with the following mean deviations: $+1.80 \pm 0.97\%$ ($3.69_5 \text{ mol kg}^{-1}$), $+3.37 \pm 2.3\%$ ($5.67_2 \text{ mol kg}^{-1}$), and $+4.05 \pm 1.5\%$ ($8.65_1 \text{ mol kg}^{-1}$).

Water activities (a_w) of the aqueous components of all the test solutions were calculated from the observed water partial pressures and are listed in Table 2. It is clear that for the fully aqueous solutions a_w varies relatively little with temperature. The ranges of water activity for these solutions are 0.8789 – 0.8967 ($3.69_5 \text{ mol kg}^{-1}$), 0.7897 – 0.8196 ($5.67_2 \text{ mol kg}^{-1}$), and 0.7019 – 0.7240 ($8.65_1 \text{ mol kg}^{-1}$). At the lowest experimental temperatures for which the test solutions contain precipitates, the water activities converge (as shown for the partial pressures in Figure 5) to a value of about 0.75 at 240 K .

4. Discussion

The ammonium bisulfate solutions studied here constitute only a single composition from the more general $(\text{NH}_4)_2\text{SO}_4$ – H_2SO_4 – H_2O system. An examination of the phase-partitioning behavior of other compositions, in addition to NH_4HSO_4 , is necessary to understand the probable cooling pathway of the test solutions. Figure 6a shows the temperatures at which NH_4HSO_4 – H_2SO_4 – H_2O mixtures are predicted to become saturated, for salt and acid molalities up to 35 mol kg^{-1} . Saturation with respect to $\text{NH}_4\text{HSO}_4(\text{cr})$ occurs over the widest range of compositions and at the highest temperatures. However, for pure aqueous NH_4HSO_4 the first precipitated solid at molalities of $\geq 6.295 \text{ mol kg}^{-1}$ and temperatures of $\geq 242.87 \text{ K}$ is predicted to be letovicite. The occurrence of sulfuric acid hydrates is restricted to very low temperatures and compositions close to pure aqueous H_2SO_4 .

Equilibrium relative humidities above the saturated solutions are shown in Figure 6b, which demonstrates that the solutions

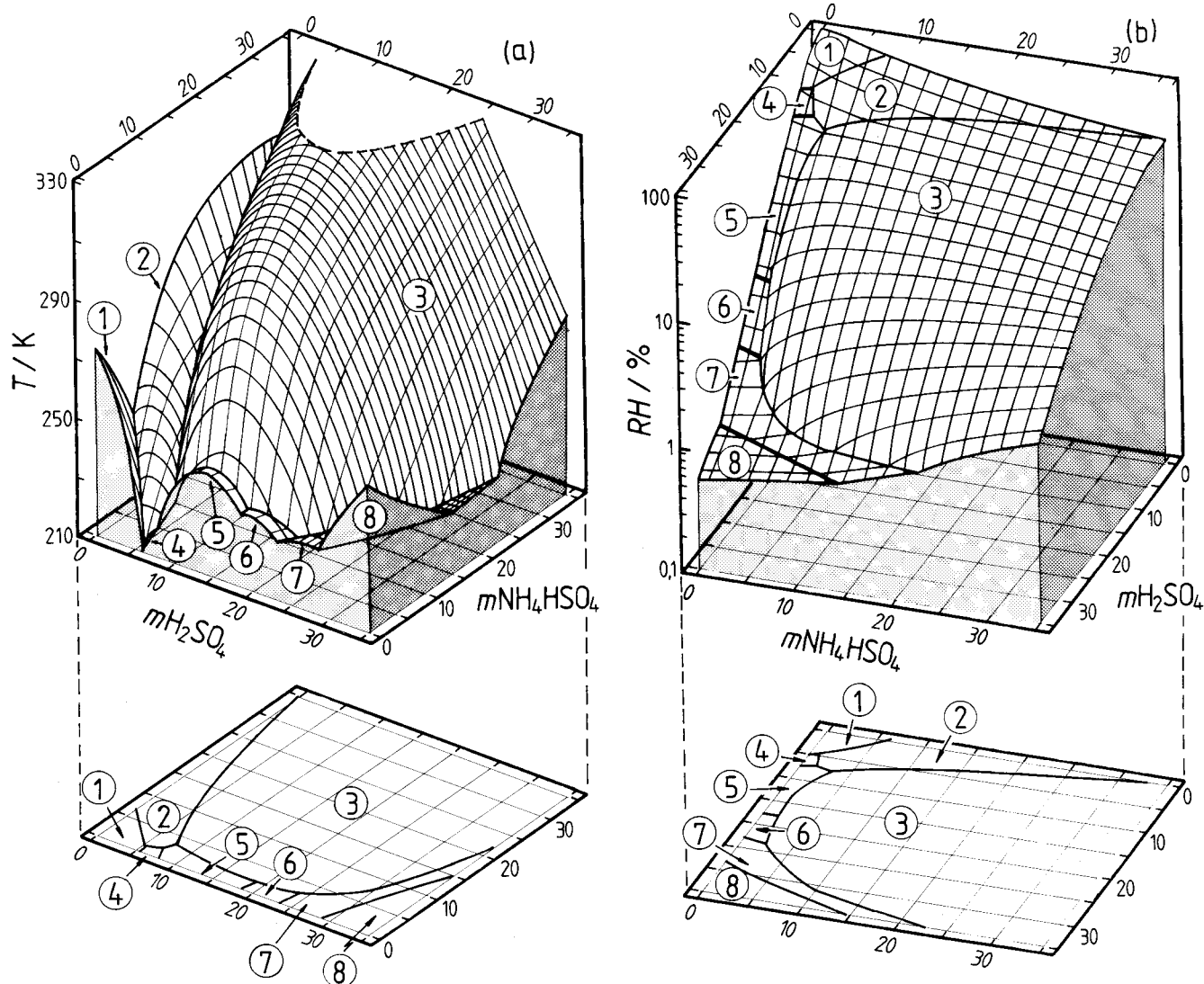


Figure 6. Calculated phase diagram of aqueous NH₄HSO₄–H₂SO₄–H₂O mixtures for 0–35 mol kg⁻¹ of each electrolyte component: (a) temperatures (*T*) at which the solutions become saturated with respect to one or more solids; (b) equilibrium relative humidities (RH) for the same temperatures and molalities as in (a). The following solids are formed: (1) ice; (2) (NH₄)₃H(SO₄)_{2(cr)}; (3) NH₄HSO_{4(cr)}; (4) H₂SO₄·6.5H₂O_(cr); (5) H₂SO₄·4H₂O_(cr); (6) H₂SO₄·3H₂O_(cr); (7) H₂SO₄·2H₂O_(cr); (8) H₂SO₄·H₂O_(cr).

containing a high proportion of NH₄⁺ become saturated at the highest relative humidities (e.g., a minimum RH of 35.3% for 35 mol kg⁻¹ NH₄HSO_{4(aq)} at 304.44 K). In contrast, solutions containing mainly H₂SO₄ remain liquid to very low relative humidities and temperatures.

We next consider the precipitation of solids from the test solutions at low temperatures, the composition of the remaining aqueous phase, and the pathway followed on the phase diagram as temperature is reduced until complete solidification occurs. Figure 7 shows a detail of the phase diagram in Figure 6, restricted to 0–9 mol kg⁻¹ NH₄HSO₄ and 0–7 mol kg⁻¹ H₂SO₄. The predicted cooling paths of the three test solutions are superimposed. First, consider the 3.69₅ and 5.67₂ mol kg⁻¹ solutions. As the solutions are initially cooled from about 293 K, a vertical path is followed (constant NH₄HSO₄ molality and zero H₂SO₄) until saturation with respect to ice is attained. Further cooling (below 258.35 K and 246.75 K, respectively) causes the precipitation of ice; the aqueous compositions move along the ice saturation curve, and the solutions become more concentrated with respect to NH₄HSO₄. This continues until saturation with respect to letovicite is reached. From this point (at 242.87 K), further cooling causes the precipitation of both

ice and letovicite and the solution composition follows the ice/letovicite boundary, becoming enriched in H⁺ relative to NH₄⁺ as the mole ratio of H⁺/NH₄⁺ becomes greater than unity. This is most easily seen in the horizontal projection in Figure 7a. The solutions are predicted to retain an aqueous component until saturation with respect to H₂SO₄·6.5H₂O_(cr) occurs at 209.29 K. At this point the aqueous phase composition is 1.06 mol kg⁻¹ NH₄HSO₄ and 5.16 mol kg⁻¹ H₂SO₄. At lower temperatures the systems exist only as a mixture of solids in the following mole ratios: H₂O_(cr)/(NH₄)₃H(SO₄)_{2(cr)}/H₂SO₄·6.5H₂O_(cr) = 1:0.0259:0.0259 (3.69₅ mol kg⁻¹ test solution) and 1:0.0438:0.0438 (5.67₂ mol kg⁻¹ test solution).

In contrast, the 8.65₁ mol kg⁻¹ test solution is predicted first to become saturated with respect to letovicite as temperature is lowered (at 261.09 K). Figure 7a shows that the aqueous composition moves into the acid region (*m*H₂SO₄ > 0 mol kg⁻¹) as precipitation of this salt occurs. At 238.50 K the solution also becomes saturated with respect to ice, and at this point the aqueous component of all three test solutions should have the same composition and same water partial pressure. The measured *p*H₂O values shown in Figure 5 are consistent with this. The 8.65₁ mol kg⁻¹ solution is predicted to become completely

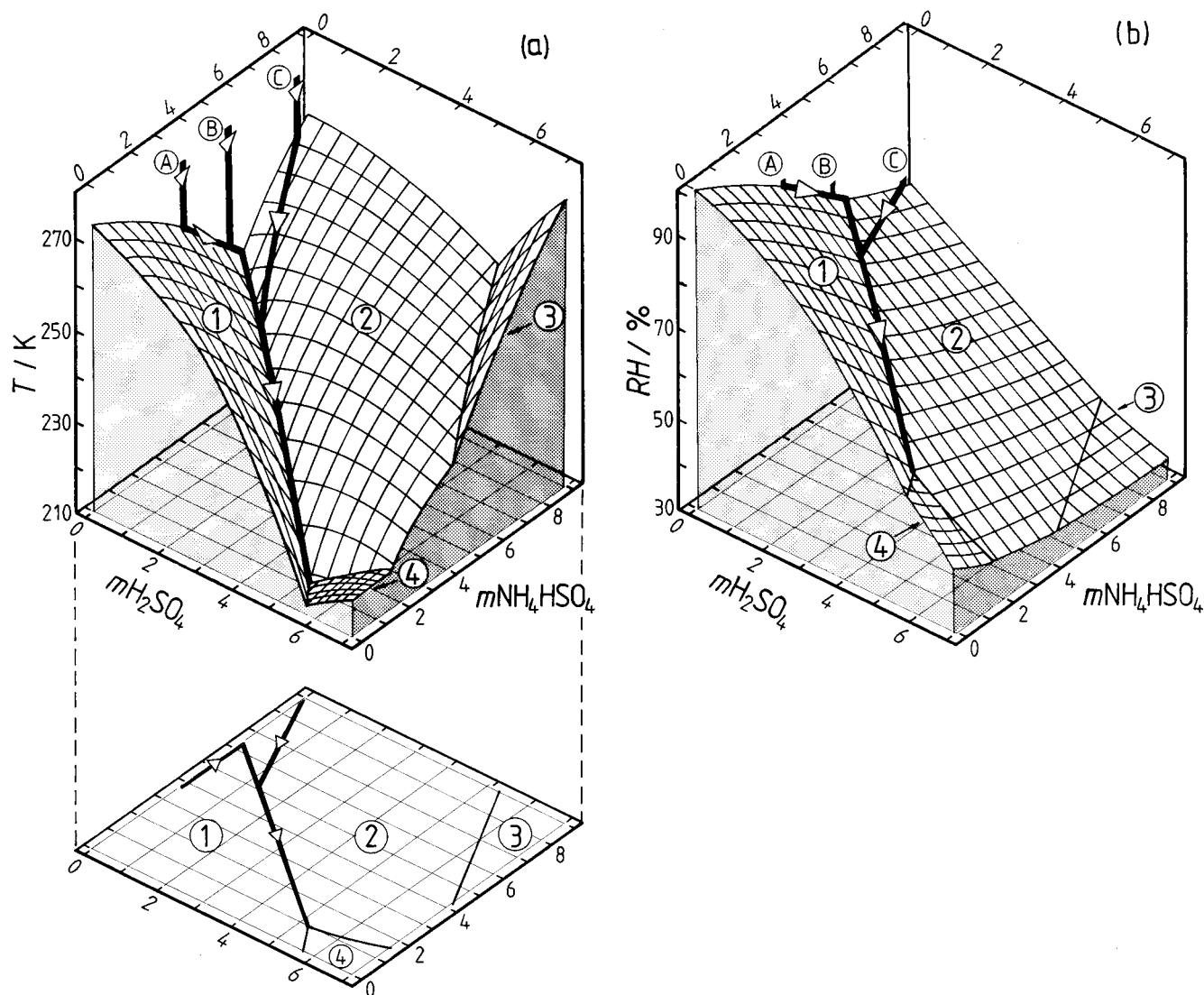


Figure 7. Cooling pathway (liquid-phase compositions as functions of temperature) of the aqueous NH_4HSO_4 test solutions, superimposed on the phase diagram of the NH_4HSO_4 – H_2SO_4 – H_2O system, from 0–9 mol kg^{-1} NH_4HSO_4 and 0–7 mol kg^{-1} H_2SO_4 : (a) temperature (T) surface; (b) equilibrium relative humidity (RH) surface. The test solutions are indicated as follows: (A) 3.69₅ mol kg^{-1} ; (B) 5.67₂ mol kg^{-1} ; (C) 8.65₁ mol kg^{-1} . The aqueous components of all three test solutions are predicted to attain the same composition at 238.5 K and complete solidification at 209.29 K. The following solids are formed: (1) ice; (2) $(\text{NH}_4)_3\text{H}(\text{SO}_4)_2(\text{cr})$; (3) $\text{NH}_4\text{HSO}_4(\text{cr})$; (4) $\text{H}_2\text{SO}_4 \cdot 6.5\text{H}_2\text{O}(\text{cr})$.

solid at 209.29 K, with the following molar composition: $\text{H}_2\text{O}(\text{cr})/(\text{NH}_4)_3\text{H}(\text{SO}_4)_2(\text{cr})/\text{H}_2\text{SO}_4 \cdot 6.5\text{H}_2\text{O}(\text{cr}) = 1:0.0785:0.0785$.

Figure 7b shows the calculated equilibrium relative humidities above the saturated solutions for the same compositions as in Figure 7a and demonstrates that the relative humidity decreases with temperature along the cooling paths of all the solutions.

Imre et al.⁴ have presented an equilibrium phase diagram for aqueous NH_4HSO_4 , based on their electrodynamic balance measurements. These are shown in Figure 8, together with predictions from the model of Clegg et al.,² our own results, and other literature data⁵ upon which the model is partially based. The work of Imre et al.⁴ yields $\text{NH}_4\text{HSO}_4(\text{cr})$ as the precipitating solid for molalities above 5.88 mol kg^{-1} (40 mass %), whereas the model predicts letovicite, which is consistent with the existing data from bulk experiments. Our own experiments also suggest letovicite as the precipitating solid, for two reasons. First, the two more dilute test solutions appeared to remain partially liquid below the temperature of saturation of aqueous NH_4HSO_4 with respect to both salt and ice. If the precipitating salt were $\text{NH}_4\text{HSO}_4(\text{cr})$, then that point would be a

eutectic and complete solidification of the solutions would be expected. Second, no ice was observed to precipitate from the 8.65₁ mol kg^{-1} solution, even at 239.56 K. This is consistent with a liquid-phase composition differing from NH_4HSO_4 stoichiometry, leading to a reduced temperature at which ice first forms (calculated to be 238.5 K; see Figure 7a).

Imre et al.⁴ observed much greater freezing point depressions (with respect to ice) than predicted by the model and determined in this work. The results of Imre et al.⁴ are compared with model calculations and data at other temperatures in Figure 9. This shows equilibrium relative humidities of 1.78–3.06 mol kg^{-1} NH_4HSO_4 calculated from the freezing point depressions in Figure 4 of Imre et al.⁴ together with values for the same compositions, as functions of temperature, calculated using the model of Clegg et al.² At 298.15 and 323.15 K the model agrees very closely with the available isopiestic data,^{10,11} which are consistent with one another and believed to be accurate. The model predicts only small variations of equilibrium relative humidity (water activity) with temperature, as would be expected for these relatively dilute solutions, and the results of Imre et

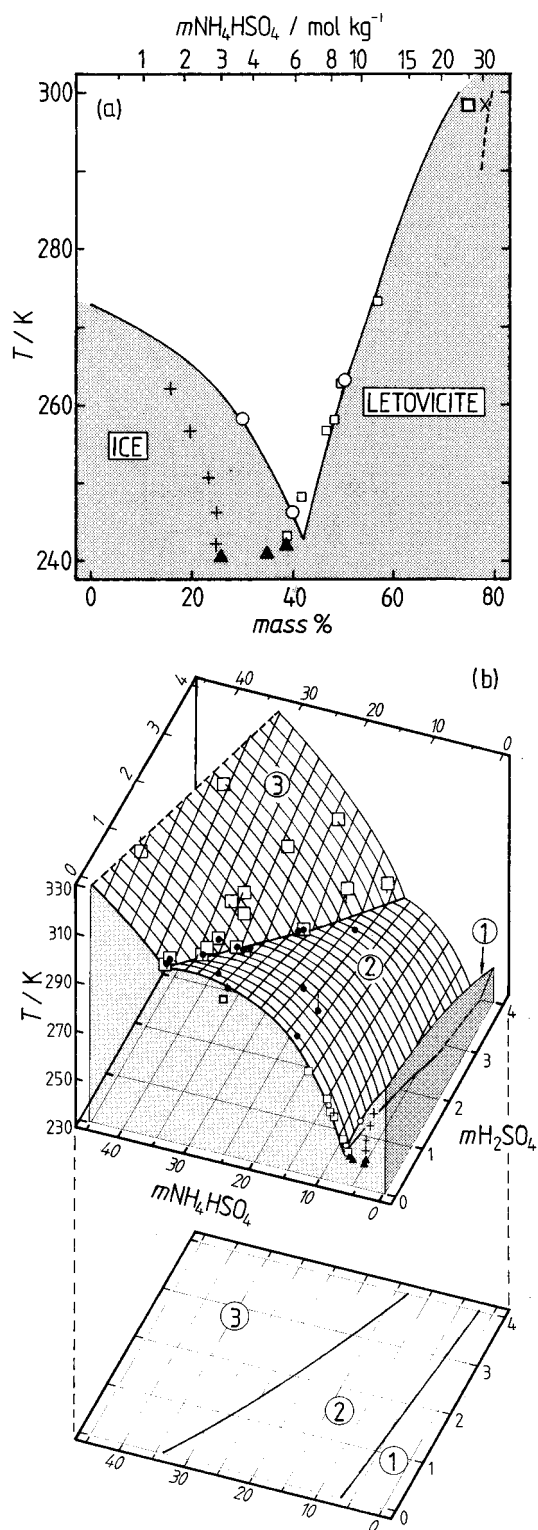


Figure 8. Measured and predicted solubilities in NH₄HSO₄-H₂SO₄-H₂O solutions. (a) Aqueous NH₄HSO₄: (+) ice (Imre et al.⁴); (▲) NH₄HSO₄·8H₂O_(cr) (Imre et al.⁴); (□) NH₄HSO_{4(cr)} (Imre et al.⁴); (bold □) NH₄HSO_{4(cr)} (Tang and Munkelwitz¹²); (○) solid (composition not determined; this study); (×) NH₄HSO_{4(cr)} (estimated from literature data⁵). Lines are from the model of Clegg et al.²: (solid) calculated ice and (NH₄)₃H(SO₄)_{2(cr)} saturation; (dashed) calculated NH₄HSO_{4(cr)} saturation. (b) NH₄HSO₄-H₂SO₄-H₂O mixtures: (+) ice (Imre et al.⁴); (▲) NH₄HSO₄·8H₂O_(cr) (Imre et al.⁴); (small □) NH₄HSO_{4(cr)} (Imre et al.⁴); (bold □) NH₄HSO_{4(cr)} (Tang and Munkelwitz,¹²); (small ○) solid (composition not determined; this study); (●) (NH₄)₃H(SO₄)_{2(cr)} (Silcock⁵); (large □) NH₄HSO_{4(cr)} (Silcock⁵). Vertical lines associated with each point from the data sets compiled by Silcock indicate the distance from the calculated surface. The following solids are formed: (1) ice; (2) (NH₄)₃H(SO₄)_{2(cr)}; (3) NH₄HSO_{4(cr)}.

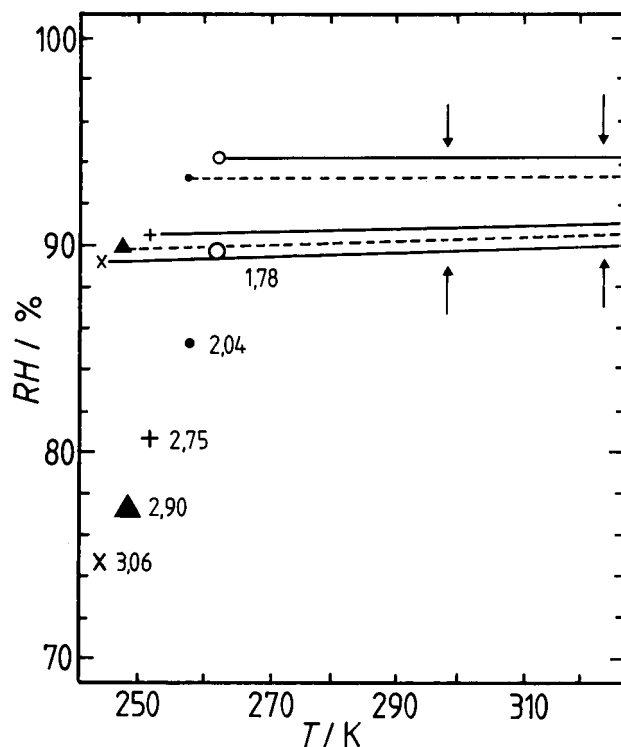


Figure 9. Comparison of equilibrium relative humidities above aqueous NH₄HSO₄. Large symbols show values derived from the freezing points of Imre et al.,⁴ at the indicated molalities (1.78–3.06 mol kg⁻¹). Small symbols and lines represent results from the model of Clegg et al.² for the same set of molalities, indicated by the symbols at the end of each line. Vertical arrows indicate the temperatures (298.15 and 323.15 K) at which the model is constrained to isopiestic data (see Clegg et al.^{2,11}).

al.⁴ are clearly inconsistent with this. It appears unlikely that it would be possible to reconcile these data with the other thermodynamic measurements available for the system.

No evidence was found in our experiments for the formation of the NH₄HSO₄·8H₂O_(cr) solid phase proposed by Imre et al.⁴ We note that, for the most dilute solution studied here, the precipitation of any hydrate with fewer than 15 molecules of water per molecule of NH₄HSO₄ would result in the remaining aqueous solution becoming more dilute with respect to NH₄HSO₄ and ultimate freezing of the solution as a mixture of hydrate and ice. Such a dilution would be inconsistent with the measured partial pressures.

The experimental results presented in this work agree well with the model of Clegg et al.² However, it is worth noting that although precipitation in the test solutions was first observed at about 258 K, a residual liquid component is predicted to remain to as low as 209.29 K, which is within the range of temperatures found in the upper troposphere. Model uncertainties increase significantly at such temperatures and are highest for solutions containing large amounts of NH₄⁺ (the H₂SO₄-H₂O system, in contrast, is relatively well characterized⁷). The magnitude of these uncertainties is difficult to assess. However, recent experiments to determine melting points of solids in the NH₄HSO₄-H₂O system suggest saturation of the liquid phase with respect to an H₂SO₄ hydrate at about 196 K (T. Koop, personal communication). While this temperature is some 13 K below that predicted by the model for saturation with respect to the hemihydrate, it is within 1 K of the temperature predicted for H₂SO₄·4H₂O_(cr) saturation. Laboratory experiments with HNO₃-H₂SO₄-H₂O mixtures suggest that this solid can form in preference to the hemihydrate under some conditions.¹³ Further measurements at very low temperature are

needed in order to define the thermodynamic properties of the system and to determine the likely atmospheric behavior of acid ammonium sulfate aerosols.

5. Summary and Conclusion

Equilibrium partial pressures of water have been measured above three aqueous NH_4HSO_4 solutions from 288.1₁ to 239.5₆ K. The temperatures at which precipitation of solids occurred were determined. In all cases the results agreed satisfactorily with predictions of the model of Clegg et al.,² including the precipitation temperatures and water partial pressures at low temperatures where the model was used also to estimate the composition of the aqueous phase.

The equilibrium phase diagram of aqueous NH_4HSO_4 shown by Imre et al.⁴ differs from that presented here chiefly in having much lower freezing points with respect to ice. Comparisons with our own measurements, which yielded precipitation at the temperatures and water vapor pressures predicted for ice by the model, suggest that the model is more nearly correct. The available literature data, the model of Clegg et al.,² and our own experiments suggest that letovicite rather than $\text{NH}_4\text{HSO}_{4(\text{cr})}$ is the equilibrium solid formed from more concentrated solutions at low temperature. Although Imre et al.⁴ obtained $\text{NH}_4\text{HSO}_{4(\text{cr})}$ in their single-particle experiments, the compositions and temperatures at which they observed saturation agree well with our own results.

Note: the thermodynamic model used to carry out the calculations presented in this work is available from S. Clegg

(s.clegg@uea.ac.uk) and can be run from the following websites: <http://www.uea.ac.uk/~e770/aim.html> and <http://www-me.udel.edu/wexler/aim.html>.

Acknowledgment. We gratefully acknowledge the support of the Natural Environment Research Council, with an Advanced Fellowship (GT5/93/AAPS/2) for Simon Clegg.

References and Notes

- (1) Seinfeld, J. H. *Atmospheric Chemistry and Physics of Air Pollution*; John Wiley and Sons: New York, 1986.
- (2) Clegg, S. L.; Brimblecombe, P.; Wexler, A. S. *J. Phys. Chem. A* **1998**, *102*, 2127–2154.
- (3) Tang, I. N.; Munkelwitz, H. R. *J. Geophys. Res.* **1994**, *99*, 18801–18808.
- (4) Imre, D. G.; Xu, J.; Tang, I. N.; McGraw, R. *J. Phys. Chem. A* **1997**, *101*, 4191–4195.
- (5) Silcock, H. L. *Solubilities of Inorganic and Organic Compounds*; Pergamon: Oxford, 1979; Vol. 3.
- (6) Massucci, M.; Clegg, S. L.; Brimblecombe, P. *J. Chem. Eng. Data* **1996**, *41*, 765–778.
- (7) Clegg, S. L.; Brimblecombe, P. *J. Chem. Eng. Data* **1995**, *40*, 43–64.
- (8) Giauque, W. F.; Hornung, E. W.; Kunzler, J. E.; Rubin, T. R. *J. Am. Chem. Soc.* **1960**, *82*, 62–70.
- (9) Wu, Y. C.; Young, T. F. *J. Res. Natl. Bur. Stand.* **1980**, *85*, 11–17.
- (10) Park, S. K.; Awakura, Y.; Majima, H. *Metall. Trans.* **1989**, *20B*, 13–20.
- (11) Clegg, S. L.; Milioto, S.; Palmer, D. A. *J. Chem. Eng. Data* **1996**, *41*, 455–467.
- (12) Tang, I. N.; Munkelwitz, H. R. *J. Aerosol Sci.* **1977**, *8*, 321–330.
- (13) Koop, T.; Biermann, U. M.; Raber, W.; Luo, B. P.; Crutzen, P. J.; Peter, Th. *Geophys. Res. Lett.* **1995**, *22*, 917–920.